CHAPTER 7
PARAMETRIC STUDY USING FINITE ELEMENT MODEL

7.1 Introduction

The finite element model developed and calibrated in Chapter 6 was used to perform a parametric study. In the parametric study, the same procedures described in Chapter 6 were used to model the construction of soil-bentonite cutoff walls, including trench excavation under a bentonite-water slurry, backfilling of the trench with soil-bentonite, and consolidation of the soil-bentonite. Various elements of the model were changed in order to evaluate the influence of existing soil conditions, soil-bentonite properties, and trench configurations on the predicted deformations. The existing soil condition was assumed to be sand of varying density and overconsolidation ratio. Other elements that were varied included, the depth of the water table, the stress-strain and compressibility properties of soil-bentonite, and the depth of the trench. The width of the trench was fixed at 3 ft. The finite element mesh and boundary conditions used in Chapter 6 and shown in Figure 6.10 was used for all analyses. The mesh represents a section of soil 200 ft deep and 580 ft long. Figure 7.1 shows a schematic of the analyzed section. The soil-bentonite trench is at the left side of the finite element mesh. The half-width of the trench is modeled, assuming symmetry on both sides of the trench.

A base case analysis was run first, assuming a normally consolidated, medium dense sand site. Typical properties for soil-bentonite and bentonite-water slurry were assumed. The results of the base case are presented in detail along with evaluation of the results. The predicted deformations in the adjacent ground and soil-bentonite cutoff wall are presented and evaluated. The final stress state of the consolidated soil-bentonite backfill is presented and evaluated. The detailed evaluation of the base case analysis indicates the following: 1) there is good confidence in the prediction of deformations in the adjacent ground, 2) the final stresses in the consolidated soil-bentonite may be too high, and 3) the settlement of the soil-bentonite may be overpredicted.

The parametric study is described after the base case. Due to the believed limitations of the finite element model, only the predicted deformations in the adjacent ground are presented. The parametric study shows what elements most influence the deformations in ground adjacent to soil-bentonite cutoff walls.

7.2 Base Case Description and Evaluation of Results

A base case analysis was run using the finite element model developed in Chapter 6. The base case was assumed to be a site of normally consolidated sand of uniform density. The depth of water was assumed to be 15 ft.

Soil Parameters used in Base Case Analysis

Sand was modeled with the Duncan and Chang (1970) hyperbolic model. Soil-bentonite was modeled using the RS model described in Chapter 4. Bentonite-water slurry was modeled with an equivalent unit weight as described in Section 6.4 and Section 6.6. The permeability of the filter cake was "smeared" into the sand elements immediately adjacent to the trench, as described in Section 6.4. The material properties used for the base case analysis are listed in Table 6.1.

The sand was assumed to be a silty sand of medium density. A hydraulic conductivity value of $1x10^{-3}$ cm/sec was assumed (Holtz and Kovacs 1981). The value of K_o was estimated from the following equation (Mayne and Kulhawy 1982) assuming an OCR value of 1 for a normally consolidated sand:

$$K_o = (1-\sin\phi') \, OCR^{\sin\phi'} \qquad (7.1)$$

The hyperbolic model parameter values were based on recommended typical parameters for a medium dense sand (Duncan et al. 1980). Slightly higher values were used than the recommended values, as these values were thought to be conservative, and may overly estimate deformations. The value of K_{ur} was assumed to be three times the estimated K value, which was found to work well for the case history modeled in Chapter 6.

Table 7.1 Soil Parameters used in Parametric Study Base Case

(a) Hyperbolic Model Parameters

Parameter	Medium Dense Sand	Medium Dense Sand Smear
Total Unit Weight (pcf)	125	125
K_o	0.43	0.43
Cohesion (psf)	0	0
Friction Angle (degrees)	35	35
Tensile Strength (psf)	0	0
R_f	0.7	0.7
K	500	500
K_{ur}	1500	1500
n	0.4	0.4
K_b	300	300
m	0.2	0.2
Hydraulic Conductivity (cm/sec)	$1.0x10^{-3}$	$3.6x10^{-6}$

(b) RS Model Parameters

Parameter	Soil-Bentonite
Total Unit Weight (pcf)	120
K_o	0.47
M	1.3
κ	0.0049
λ	0.07
Poisson's Ratio	0.32
N (for pressure in psf)	1.044
R	2.01
S	2.01
Hydraulic Conductivity (cm/sec)	$1.0x10^{-7}$

(c) Linear Elastic Model Parameters

Parameter	Soil-Bentonite During Fill Step
Total Unit Weight (pcf)	120
K_o	0.99203
Young's Modulus (psf)	0.01
Poisson's Ratio	0.498
Initial Vertical Effective Stress (psf)	100
Hydraulic Conductivity (cm/sec)	$1.0x10^{-7}$

(d) Bentonite-Water Slurry Data

Parameter	Bentonite-Water Slurry
Total Unit Weight (pcf)	75

The soil-bentonite and bentonite-water slurry properties in Table 7.1 were chosen to be representative properties based on information on soil-bentonite cutoff walls presented in Chapter 2 and Chapter 3.

Procedures for Base Case Analysis

The steps used to model the base case analysis are listed in Table 7.2. The procedures for each step are described in full detail in Section 6.6, and are only briefly summarized here. The initial stresses were assigned using the unit weight and K_o value for sand from Table 7.1. The pore pressures were assigned using a water table at 15 ft, and assuming negative pore pressures above the water table. As discussed in Section 6.4, negative pore pressures were necessary in order to accurately model the consolidation of the soil-bentonite. Total head boundary conditions were assigned to the right side of the finite element mesh to correspond to a constant head of 185 ft (using a datum at the bottom of the finite element mesh). The trench was excavated by removing elements of sand in the trench and applying a pressure to the trench walls and trench bottom equal to the pressure from the bentonite-water slurry. The trench was backfilled by placing rows of soil-bentonite starting from the bottom of the trench. The bentonite-water slurry pressure was removed as the slurry was replaced with soil-bentonite. The pore pressures in the filled elements were assigned by assuming that the initial vertical effective stress in the just placed soil-bentonite is approximately 100 psf. After backfilling, the excess pore pressures in the soil-bentonite were allowed to dissipate during a number of consolidation steps. One year of consolidation was modeled, which was enough time to dissipate excess pore pressures.

Table 7.2 Steps for Modeling Base Case

Sequence	Time for Each Sequence (days)	Step Numbers
Assign initial stresses	NA	0
Apply head boundary conditions	0.2	1
Excavate trench under bentonite-water slurry	8	2
Backfill trench, replacing bentonite-water slurry with soil-bentonite	20	2-22
Consolidation only	365	23-25

A new procedure was introduced after evaluating the preliminary results of the base case analysis. The calculated lateral deformations with depth after excavation are shown in Figure 7.2. The deformations are plotted at a distance of 27 ft from the trench centerline. The calculated lateral deformations brought to light an undesirable effect of assuming negative pore pressures above the water table.

The effect of assuming negative pore pressures above the water table on the total horizontal stresses is illustrated in Figure 7.3, which is series of plots of stresses at the trench wall. Figure 7.3a shows the pore pressures in the sand with and without negative pore pressures above the water table. Stresses assuming negative pore pressures are illustrated by a solid line in all plots, and stresses without negative pore pressures are indicated by a dashed line in all plots. Figure 7.3b shows the total vertical stress in the sand, assuming that the vertical stress is a principal stress. Figure 7.3c shows the effective vertical stress in the sand with and without negative pore pressures. Figure 7.3d shows the effective horizontal stress in the sand calculated using the K_o value in Table 7.1. Figure 7.3e shows the total horizontal stress in the sand. It can be seen in Figure 7.3e that assuming negative pore pressures results in negative total horizontal stress in some places above the water table in the sand. This would mean that if the trench were excavated even without a slurry to support the trench, the top part of the trench would move back into the forma-

tion as a result of the excavation. Since this was not considered reasonable behavior, a pressure was applied to the excavation face equal to the difference in total horizontal stresses with negative pore pressures and without negative pore pressures. The difference is shown in Figure 7.3f to an exaggerated scale. The difference can be calculated from the following equation:

$$\sigma_h = (1-K_o)\,\gamma_w\,h \qquad (7.2)$$

where:

σ_h = horizontal pressure to apply to face of excavation

K_o = Lateral earth pressure coefficient at rest in existing sand

γ_w = unit weight of water

h = height above water table (a positive value)

This pressure was applied at the trench wall, pushing inward toward the trench centerline. In this way, the effect of negative pore pressures on the total horizontal stress was counteracted. The total horizontal stress in the sand is opposed by the pressure from the bentonite-water slurry, which is shown in Figure 7.3g. The net pressure distribution at the trench wall resulting from excavation under bentonite-water slurry is shown in Figure 7.3h by the dashed line above the water table and the solid line below the water table. The pressures from equation 7.2 were removed as the trench was filled with soil-bentonite so that equilibrium was restored. With this new procedure, a final analysis of the base case was performed.

In Figure 7.4, the predicted lateral deformations after excavation from the final analysis of the base case are compared with the preliminary analysis. The figure shows that more inward lateral movement is predicted due to applying the pressure shown in Figure 7.3f (equation 7.2) to the trench wall. The final analysis predicts greatest inward lateral deformation near the bottom of the trench and smaller outward deformation nearer to the top of the trench. The final predicted lateral movement is consistent with the net pressure diagram shown in Figure 7.3h. The net pressure diagram shows a net pressure pushing

the trench wall toward the trench centerline (positive $\Delta\sigma_x$) at the bottom of the trench, and a smaller net pressure pushing the trench wall away from the trench centerline (negative $\Delta\sigma_x$) at around 15 ft depth.

Evaluation of Predicted Deformations

The incremental lateral deformations for the base case analysis are shown for each construction phase in Figure 7.5 with the solid lines. The deformations are plotted at a distance of 27 ft from the trench centerline in order to compare the results of the base case to the analysis of the Raytheon case history. The deformations predicted for the Raytheon case history are shown in the figure with the dashed lines.

After excavation, the lateral deformations in adjacent ground for the base case analysis indicate the greatest inward movement at a depth of about 70 ft and less inward movement near the ground surface. This trend is explained by the net horizontal pressure at the trench wall due to excavation, as discussed in the previous section. For modeling of the Raytheon case history, an inward lateral movement was predicted with the largest magnitude at the ground surface. The difference can be explained by a higher unit weight slurry used for the base case, and a lower K_o for the existing sand for the base case. Both of these conditions would produce less net pressure pushing into trench (toward the trench centerline), and less inward movement.

During the backfilling phase, a maximum of about 3/4 inch of additional inward lateral deformation is predicted. The maximum deformation occurs at the ground surface. At the Raytheon site, very small outward deformations were predicted during the backfilling phase. It is thought that more consolidation of the soil-bentonite occurs during excavation for the base case analysis due to higher permeability soils adjacent to the trench. The base case analysis has sand of higher permeability compared to lower permeability sand and clay at the Raytheon site. The consolidation of the soil-bentonite causes inward lateral movement. This overshadows the effect of replacing the bentonite-water slurry

with the higher density soil-bentonite, which would cause outward lateral movement.

During consolidation, an maximum additional 1/2 inch of lateral deformation is predicted for the base case. The maximum deformation occurs at the ground surface. The incremental deformation during consolidation for the Raytheon site is 3/4 inch. The shapes of the deformation with depth are similar for both analyses.

The total lateral deformations at the end of each phase are shown in Figure 7.6 for the base case analysis. The predicted lateral deformation at the ground surface is approximately 0 inch, 3/4 inch, and 1 1/4 inch of inward deformation at the end of excavation, backfilling, and consolidation. Very little deformation occurs below the bottom of the trench.

The total settlement at the ground surface at the end of each construction phase is shown as a function of distance from the trench centerline in Figure 7.7. Also shown in the figure is the total horizontal deformation at the ground surface as a function of distance from the trench centerline. The settlement plot shows that settlement increases with each phase of construction, and a similar trend is predicted for the lateral deformation. Very little deformation is predicted during the excavation phase. Most of the deformations occur during and after backfilling. The most ground settlement occurs nearest the trench and decreases with distance from the trench. The predicted settlement becomes less than 1/4 inch at a distance of about 150 ft from the trench centerline. The horizontal deformation plots indicate that the deformation is approximately constant to a distance of 50 ft from the centerline of the trench. Beyond a distance of 50 ft, the horizontal deformations decrease, and the deformations become less than 1/4 inch after about 200 ft. The model predicts similar or slightly greater horizontal deformations than settlement. In general, deformations in the adjacent ground appear reasonable, and are similar in nature to measured deformations shown in Sections 2.4 and 6.7.

The calculated settlement in the trench is shown in Figure 7.8. About 3 ft of settlement was predicted to occur near the center of the trench, while an inch is predicted in the sand at the trench wall. The maximum predicted settlement in the trench is 3% of the height of the trench, which may seem excessive, but is within the range of values reported in Section 2.4. Settlement in two soil-bentonite trenches were reported as 0.1% and 3-4% for 3 ft wide trenches. Mostly uniform settlement of the soil-bentonite is predicted in the trench, with most of the differential settlement between the soil-bentonite and the existing sand occurring in the thin soil-bentonite element next to the trench wall.

A simple 1-D calculation was preformed to calculate the settlement in the trench if no shear stresses developed at the trench wall and the soil-bentonite was fully consolidated under self weight. Assuming the initial stress of the soil-bentonite to be 100 psf, the estimated 1-D consolidation in the trench is calculated to be 13.2 ft. The calculated settlement from the finite element analyses is much less due to shear stresses in the soil-bentonite and adjacent sand, and consolidation that occurs during soil-bentonite placement.

In general, there is good confidence in predicted deformations in adjacent ground. The deformations are similar to the analysis of the Raytheon case history, which was calibrated using measured lateral deformations and settlement data. Large settlement is predicted in the trench, which is within the range of reported values for other cutoff walls. Large differential deformations occur in the soil-bentonite element nearest the trench. These elements are further examined later in this section.

Evaluation of Predicted Stresses in Consolidated Soil-Bentonite

There are three rows of elements representing the soil-bentonite in the finite element mesh. Together, the three columns are 1.5 ft wide, representing the half-width of the trench. The first column, nearest the trench centerline, is 0.75 ft wide. The second column is 0.45 ft wide, and the third column is 0.30 ft wide. The calculated effective

vertical stress, σ_y', in the consolidated soil-bentonite for each column is shown in Figure 7.9. The values of σ_y' with depth are similar for the first two columns of soil-bentonite. The values of σ_y' are smaller for the third column, which is next to the trench wall. The predicted effective vertical stress increases with depth. The values of σ_y' for geostatic conditions, lateral squeezing theory, and arching theory are also shown on the figure. The predicted stresses are less than geostatic stresses and greater than both the lateral squeezing and arching theories.

The calculated effective horizontal stress, σ_x', with depth is shown in Figure 7.10. The calculated effective horizontal stresses are less than the calculated effective vertical stresses. The first two columns have similar effective horizontal stresses, which are greater than effective horizontal stress in the third column. The values of σ_x' for geostatic conditions, lateral squeezing theory, and arching theory are also shown on the figure. The σ_x' stresses in the first two columns are less than the geostatic stresses, but greater than the lateral squeezing and arching theories. The values of σ_x' in the third column are less than geostatic and lateral squeezing stresses, and greater than arching theory.

The effective horizontal stresses in the third column are thought to be too low when compared to the two other columns. The elements in the third column are very thin and the shear stresses in the elements are not great enough to explain the large difference in horizontal stresses from the second to the third column. Total horizontal force equilibrium does not seem to be met for the third column. Horizontal force equilibrium does seem to be met for the column of sand next to the trench and the first two columns of soil-bentonite.

The average stresses calculated in the soil-bentonite indicated that none of the soil-bentonite elements were at failure. However, in the third column of soil-bentonite elements, the two gauss points closest to the trench wall were at failure over most of the

depth of the trench. The final stresses at the gauss points from nine elements are shown in Figure 7.11. The gauss points from a row of elements near the top of the trench are plotted, along with the gauss points from a row of element near the middle of the trench, and a row of elements near the bottom of the trench. Each row has three elements, and each element has four gauss points. The six gauss points nearest the trench wall are plotted with open symbols, whereas the other gauss points are plotted with closed symbols. The figure shows that the six gauss points nearest the trench wall are at failure. The six gauss points at failure are clustered together on the failure line and have much lower deviatoric stresses than the rest of the gauss points. The other gauss points in the third column of elements, and in the other columns of elements are not at failure. The figure also shows that the gauss points towards the bottom of the trench have in general, higher deviatoric stresses than the gauss points towards the top of the trench.

It is thought that due to failure of the gauss points near the trench wall, the shear and normal stresses in the third column of soil-bentonite elements are too low. These gauss points failed early in the consolidation process while the effective normal stresses were quite low. Evidently, the finite element program was not able to track gauss points up the failure line if normal stresses are increased after failure. If interface elements had been available for use in this finite element model, perhaps the stresses could have been modeled more accurately. As described in Section 6.6, problems were encountered with the interface elements and their use had to be abandoned.

As a result of the failure of some of the gauss points in the soil-bentonite elements, it is thought that the shear stresses are too low in the soil-bentonite. Since the shear stresses were not able to transmit enough load to the adjacent sand, the vertical effective stresses calculated in the soil-bentonite are thought to be too high. Presently, there is no data available to calibrate the results of the consolidated stresses in the soil-bentonite.

Due to the uncertainty of the results of the effective stresses in the third column of soil-bentonite elements, the accuracy of the deformations predicted in this column and the settlement in the trench are uncertain.

Summary of Evaluation of Results

Calculated deformations in the adjacent ground for the base case analyses exhibit similar trends to those for the calibrated case history from Chapter 6. Therefore, confidence in the deformations in the adjacent ground are relatively good, and they are reported for the parametric study. Since the effective stresses in the consolidated soil-bentonite are thought to be too high, the predicted stresses in the soil-bentonite and the settlement of the soil-bentonite in the trench are not reported for the parametric study.

7.3 Description of Parametric Study

Various elements of the base case analysis were changed in order to evaluate the influence of existing soil conditions, soil-bentonite properties, and trench configurations on the predicted deformations in adjacent ground.

The following items were varied:

1) Trench depth
2) Sand density
3) Sand OCR
4) R value of soil-bentonite
5) λ value of soil-bentonite
6) Depth of water table

A summary of the computer runs for the parametric study is shown is Table 7.3. The base case analysis is listed as case number 1. The procedures used in the modeling are described in Chapter 6. Changes or new procedures that were used in the parametric study are described in the following paragraphs when appropriate.

Table 7.3 Summary of Parametric Study

Case Number	Trench Width (ft)	Trench Depth (ft)	Sand Properties		Soil-Bentonite Properties				Water Depth (ft)
			Sand Density	Sand OCR	R	S	λ	κ	
1	3	100	Medium	1	2	2	.07	.0049	15
2	3	30	Medium	1	2	2	.07	.0049	15
3	3	60	Medium	1	2	2	.07	.0049	15
4	3	100	Loose	1	2	2	.07	.0049	15
5	3	100	Dense	1	2	2	.07	.0049	15
6	3	100	Loose	2	2	2	.07	.0049	15
7	3	100	Medium	2	2	2	.07	.0049	15
8	3	100	Dense	2	2	2	.07	.0049	15
10	3	100	Medium	1	4	2	.07	.0049	15
11	3	100	Medium	1	3	2	.07	.0049	15
12	3	100	Medium	1	2	2	.03	.0021	15
13	3	100	Medium	1	2	2	.10	.007	15
14	3	100	Medium	1	2	2	.07	.0049	10
15	3	100	Medium	1	2	2	.07	.0049	20

Cases 2 and 3 were performed to investigate the effect of trench depth. The trench depth was changed to 30 and 60 ft. The width of the trench was constant at 3 ft for all runs. The construction times for a 30 ft and 60 ft trench were calculated from typical soil-bentonite construction rates estimated by a geotechnical engineer who works for a specialty contractor (Burke 1999). Much shorter times were estimated for the 30 ft and 60 ft trench than for the 100 ft trench, since it was assumed that the shorter trenches could be excavated with a backhoe, while a clam shell would be required for a 100 ft trench.

Cases 4 and 5 were performed to investigate the effect of sand density. The sand density was varied from medium to loose and dense. The sand was assumed to be normally consolidated. The effect of overconsolidation of the sand was investigated in cases 6 through 8. An OCR of 2 was assumed for sites with loose, medium, and dense sand. The hyperbolic model parameter values that were assumed for each sand are listed in Table 7.4. For the purposes of this study, it was assumed that the only affect of overconsolidation on material property values was to increase the value of K_o according to equation

7.1. Also, the effect of overconsolidation was modeled by applying and removing a surcharge of 2814 psf to the entire site. It was estimated that this pressure would cause an OCR close to 2 over about 80% of the depth of the analyzed section.

Table 7.4 Soil Parameter Values for Sand used in Parametric Study

Hyperbolic Model Parameter	NC Loose Sand	NC Medium Sand	NC Dense Sand	OC Loose Sand	OC Medium Sand	OC Dense Sand
OCR	1	1	1	2	2	2
Total Unit Weight (pcf)	120	125	135	120	125	135
K_o	0.5	0.43	0.36	0.71	0.63	0.56
Cohesion (psf)	0	0	0	0	0	0
Friction Angle (degrees)	30	35	40	30	35	40
Tensile Strength (psf)	0	0	0	0	0	0
R_f	0.7	0.7	0.7	0.7	0.7	0.7
K	250	500	1000	250	500	1000
K_{ur}	750	1500	3000	750	1500	3000
n	0.4	0.4	0.4	0.4	0.4	0.4
K_b	150	300	450	150	300	450
m	0.2	0.2	0.2	0.2	0.2	0.2

notes: NC = Normally Consolidated, OC = Overconsolidated

The effect of the R parameter for soil-bentonite was investigated in cases 10 and 11. The R value was varied to 3 and 4. An R value of 2 was used for the base case analysis. The R value was found to be 4 for soil-bentonite mixtures SB1 and SB3, and the value of R was found to be 2 for the soil-bentonite at the Raytheon site. The effect of varying λ and κ of the soil-bentonite was investigated in cases 12 and 13. The λ value was varied to 0.03 and 0.10. The range of reported values of λ was estimated to be 0.2 to 0.11 from data reported in Chapter 2 and 3. The κ value was varied accordingly, assuming a λ/κ relationship of 0.07. This ratio of λ/κ was found to be a typical value from data presented in Chapter 2 and 3.

In cases 14 and 15 the depth of the water table was varied from 10 to 20 ft. The values of water depth were chosen such that the water table was as high as possible, but that the

factor of safety estimated for trench stability during excavation was greater than 1.2 for all runs. The factors of safety were calculated using equations established for excavation of soil-bentonite trenches under bentonite-water slurry assuming planar slip surfaces in sand (Adams et al. 1997).

7.4 Results of the Parametric Study

Deformations in Adjacent Ground

The results of the parametric study are shown in Figures 7.12 to 7.19. The figures show the predicted settlement and horizontal deformation in the adjacent ground at the ground surface for all cases. Figures 7.12 through 7.19 show the effect of trench depth, sand density, OCR for loose sand, OCR for medium sand, OCR for dense sand, soil-bentonite R value, soil-bentonite λ value, and depth of water, respectively.

The figures show that the patterns of settlement and lateral deformation are similar for all cases. The maximum predicted settlement typically occurs at the trench wall and gradually decreases with distance. The lateral displacement is approximately constant over the 50 ft closest to the trench for 100 ft trenches. The lateral displacement decreases at greater distances from the trench. The graphs show that most of the deformation occurs within 200 ft of the trench centerline, and this region has the greatest differential settlement. The figures also show significant deformations (greater than 1/4 inch) at distances of 100 to 290 ft for all cases with 100 ft deep trenches (all cases except 2 and 3).

The maximum settlement and maximum lateral deformation for each case are summarized in Table 7.5. For each series, the maximum deformations are compared to a baseline case. The base line case is listed first in each series and is typically the base case analysis. For the series of overconsolidated sands, the base line is considered the normally consolidated site. For example, in the trench depth series, the base line case is Case 1, the base case analysis. The table shows that when the trench was varied from 100 ft in depth to 30 ft in depth, the maximum settlement (max) decreased from 1.19 inch

to 0.07 inch. The table shows the difference in settlement from the base line (Δ) is –1.12 inch. The percent difference from the base line (% change) is -94%.

Table 7.5 Summary of Maximum Deformations in Adjacent Ground for Parametric Study

Case	Description	Settlement			Lateral Deformation		
		max (in.)	Δ (in.)	% change	max (in.)	Δ (in.)	% change
1	100 ft trench depth	1.19	NA	NA	1.37	NA	NA
2	30 ft trench depth	0.07	-1.12	-94	-.08	-1.45	-106
3	60 ft trench depth	0.43	-0.76	-64	0.42	-.95	-69
1	Medium NC sand	1.19	NA	NA	1.37	NA	NA
4	Loose NC sand	2.69	1.50	126	3.05	1.68	123
5	Dense NC sand	0.67	-0.52	-44	0.87	-.50	-36
4	Loose NC sand	2.69	NA	NA	3.05	NA	NA
6	Loose OC sand	3.55	0.86	24	4.45	1.40	31
1	Medium NC sand	1.19	NA	NA	1.37	NA	NA
7	Medium OC sand	1.73	0.54	31	2.18	0.81	37
5	Dense NC sand	0.67	NA	NA	0.87	NA	NA
8	Dense OC sand	0.97	0.30	31	1.22	0.35	29
1	Soil-bentonite R=2	1.19	NA	NA	1.37	NA	NA
11	Soil-bentonite R=3	1.23	0.04	3	1.48	0.11	8
10	Soil-bentonite R=4	1.26	0.07	6	1.57	0.20	15
1	Soil-bentonite λ=0.07	1.19	NA	NA	1.37	NA	NA
12	Soil-bentonite λ=0.03	0.65	-0.54	-45	0.70	-0.67	-49
13	Soil-bentonite λ=0.10	1.47	0.28	24	1.72	0.35	26
1	Water table 15 ft	1.19	NA	NA	1.37	NA	NA
14	Water table 10 ft	1.98	0.79	66	2.30	0.93	68
15	Water table 20 ft	0.79	-0.40	-34	0.91	-0.46	-34

The parametric study indicates the following trends. Decreasing the depth of the trench decreases the deformations. Decreasing the density of the sand, increases the deformations. Increasing the OCR of the sand increases the deformations. Increasing the R value of soil-bentonite increases the deformations. Increasing the λ value of soil-bentonite increases the deformations. Lowering the water table decreases the deformations.

The results of the parametric study indicate that changing the density of the sand has the greatest effect on the magnitudes of deformations compared to the base case analysis. The next greatest effect is caused by varying the depth of the trench, followed by depth of water, soil-bentonite λ value, sand OCR, and soil-bentonite R value. The parametric study indicates that changing the R value of soil-bentonite has very little effect on deformations in adjacent ground. The parametric study indicates that changing the OCR from 1 to 2 has greatest effect on the magnitude of deformations for loose sands and the smallest effect on the magnitude of deformations for dense sands. The percent change in the deformations is about the same for changing the OCR from 1 to 2 regardless of soil density.

Factor of Safety During Excavation

The factor of safety, FS, against trench stability during excavation can be calculated for several of the cases in the parametric study. Closed form solutions assuming planar slip surfaces in sand (Adams et al. 1997) were used. The factor of safety is a function of 1) ratio of height of water table to depth of trench, 2) ratio of height of bentonite-water slurry in trench to depth of trench, 3) unit weight of bentonite-water slurry and, 4) unit weight of sand and friction angle of sand. Factors of safety were calculated for cases 1, 2, 3, 4, 5, 14, and 15. For these cases, the height of the water table was varied, the depth of trench was varied, the unit weight of sand was varied and the friction angle of the sand was varied. The height of the bentonite-water slurry was assumed to be equal to the depth of the trench in all cases. The unit weight of the bentonite-water slurry and the soil-bentonite properties were not varied for these cases. The factor of safety values are shown in Table 7.6. The factor of safety for cases 12 and 13 are also shown in Table 7.6. In these cases, the compressibility of the soil-bentonite was varied by changing the λ parameter.

The values of factors of safety were compared to the normalized maximum settlement after excavation and consolidation. The maximum settlement values after excavation and

consolidation were normalized by the depth of the trench. The settlement values are shown in Table 7.6.

Table 7.6 Factor of Safety During Excavation and Maximum Settlement Values After Excavation and Consolidation

Case	Description	FS	$Sett_{exc}$ (inch)	$Sett_{exc}$ / H x 100 %	$Sett_{con}$ (inch)	$Sett_{con}$ / H x 100 %
1	100 ft trench depth	1.37	0.16	0.013	1.19	0.099
2	30 ft trench depth	2.26	-0.03	-0.009	0.07	0.019
3	60 ft trench depth	1.68	-0.05	-0.006	0.43	0.060
4	Loose CD sand	1.21	0.90	0.075	2.69	0.224
5	Dense NC sand	1.45	0.02	0.002	0.67	0.056
14	Water table 10 ft	1.20	0.48	0.040	1.98	0.165
15	Water table 20 ft	1.53	-0.07	-0.006	0.79	0.066
12	Soil-bentonite λ=0.03	1.37	0.16	0.013	0.65	0.054
13	Soil-bentonite λ=0.10	1.37	0.16	0.013	1.47	0.122

Notes: FS = Factor of safety during excavation
$Sett_{exc}$ = Maximum settlement of adjacent ground after excavation
H = Trench depth
$Sett_{con}$ = Maximum settlement of adjacent ground after consolidation

The factors of safety are plotted versus normalized maximum settlement after excavation in Figure 7.20a with open triangles pointing down. Figure 7.20a indicates that there is a trend of increasing normalized settlement after excavation with decreasing factor of safety during excavation, as expected. The factors of safety are plotted versus normalized maximum settlement after consolidation in Figure 7.20b. Figure 7.20b indicates that there is also a trend of increasing normalized settlement after consolidation with decreasing factor of safety during excavation. Cases 1, 2, 3, 4, 5, 14, and 15 are plotted in Figure 7.20b with open circles. In all of these cases the soil-bentonite has the same property values including λ=0.07. In Figure 7.20b a trend line was estimated for the normalized settlement after consolidation for the seven cases with λ=0.07 as shown by the solid line. Trend lines were also estimated for λ=0.03 and λ=0.10 from cases 12 and 13 as shown by the dashed line and dash-dot line, respectively.

Figure 7.20b incorporates many factors that were shown to be significant on the settlement in adjacent ground from the parametric study. Changes in properties of the sand, water table depth, and trench depth are incorporated with the factor of safety, and changes in soil-bentonite compressibility are incorporated the with the trend lines for various λ values. It should be noted that the figure is based on a 3 ft wide trench.

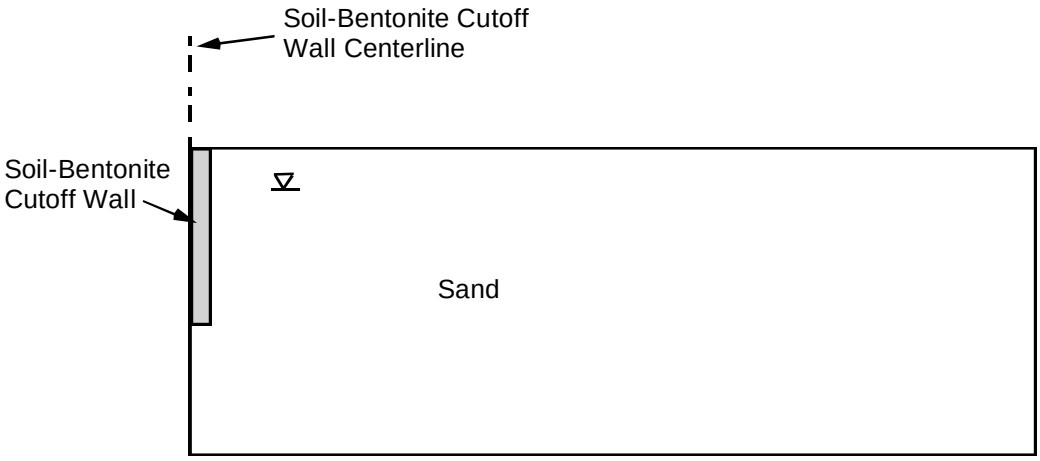

Figure 7.1 Section Analyzed in Parametric Study

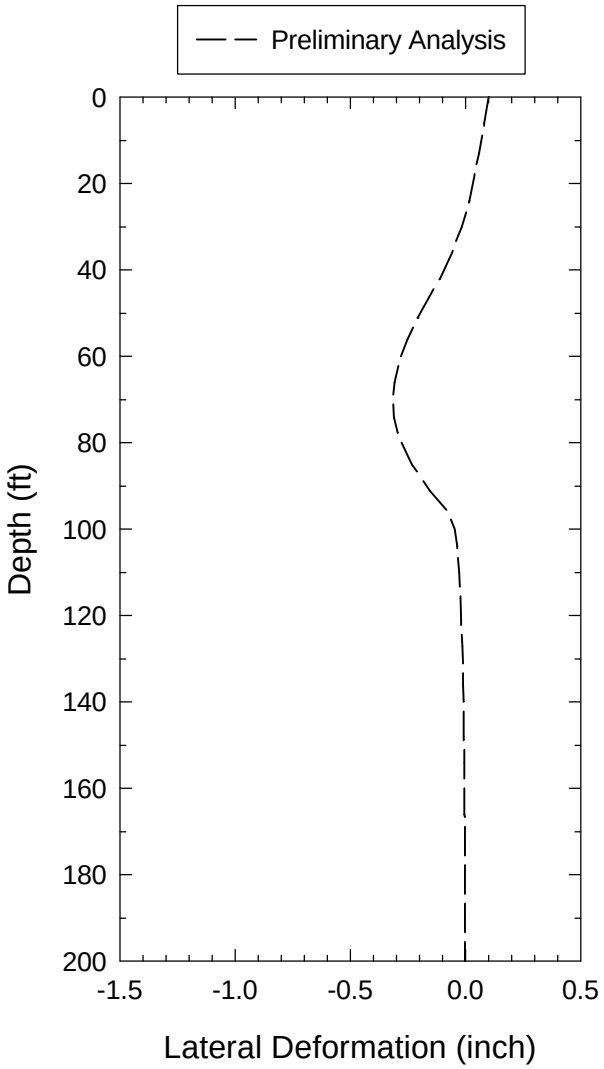

Note: Negative Deformation = Toward Trench Centerline

Figure 7.2 Preliminary Analysis: Predicted Lateral Deformations after Excavation

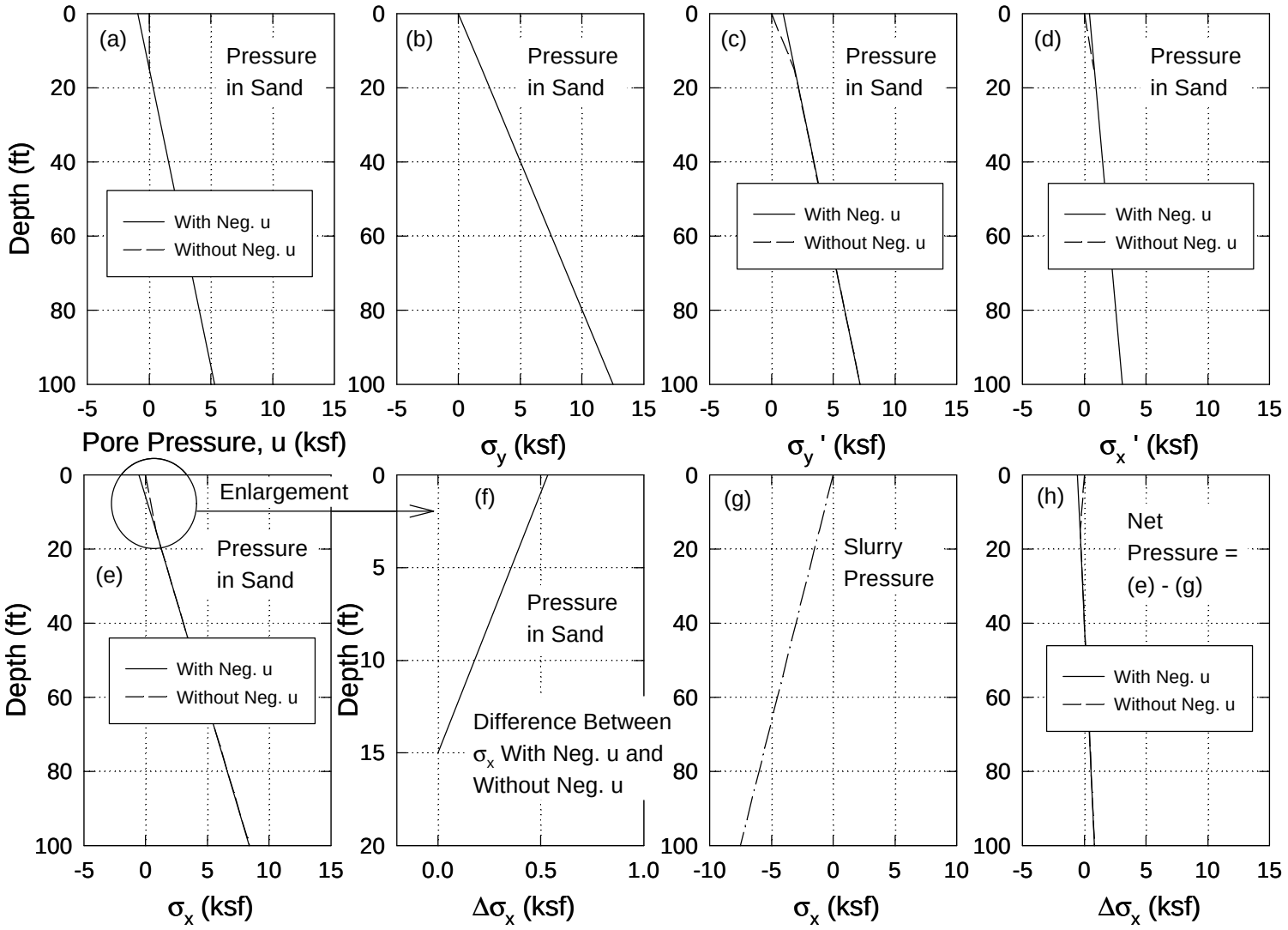

Figure 7.3 Pressures at Trench Wall with Depth for Base Case Analysis

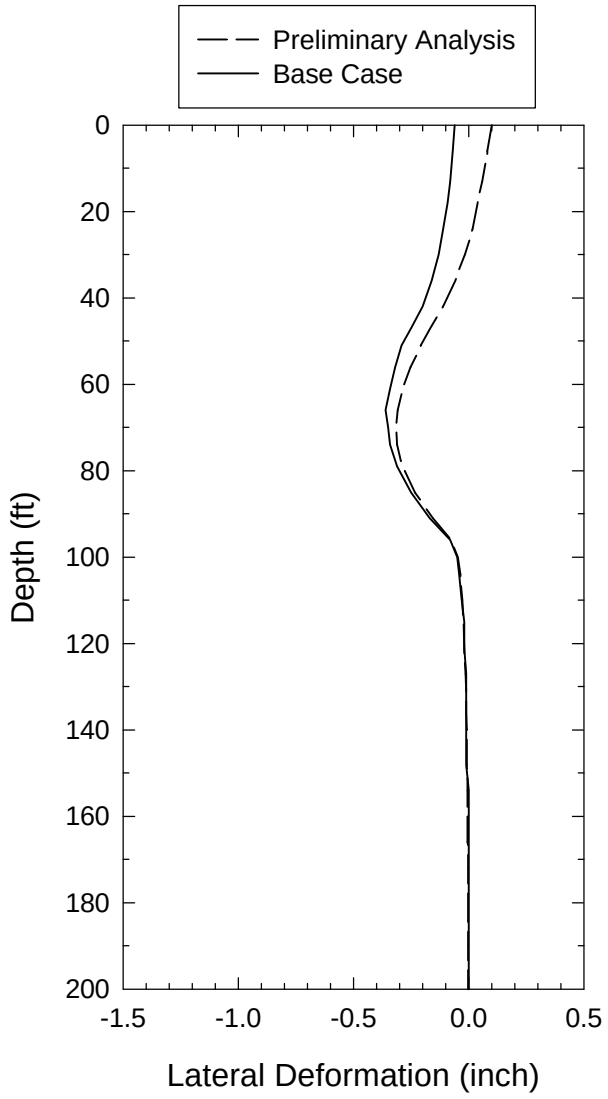

Note: Negative Deformation = Towards Trench Centerline

Figure 7.4 Base Case: Predicted Lateral Deformations after Excavation

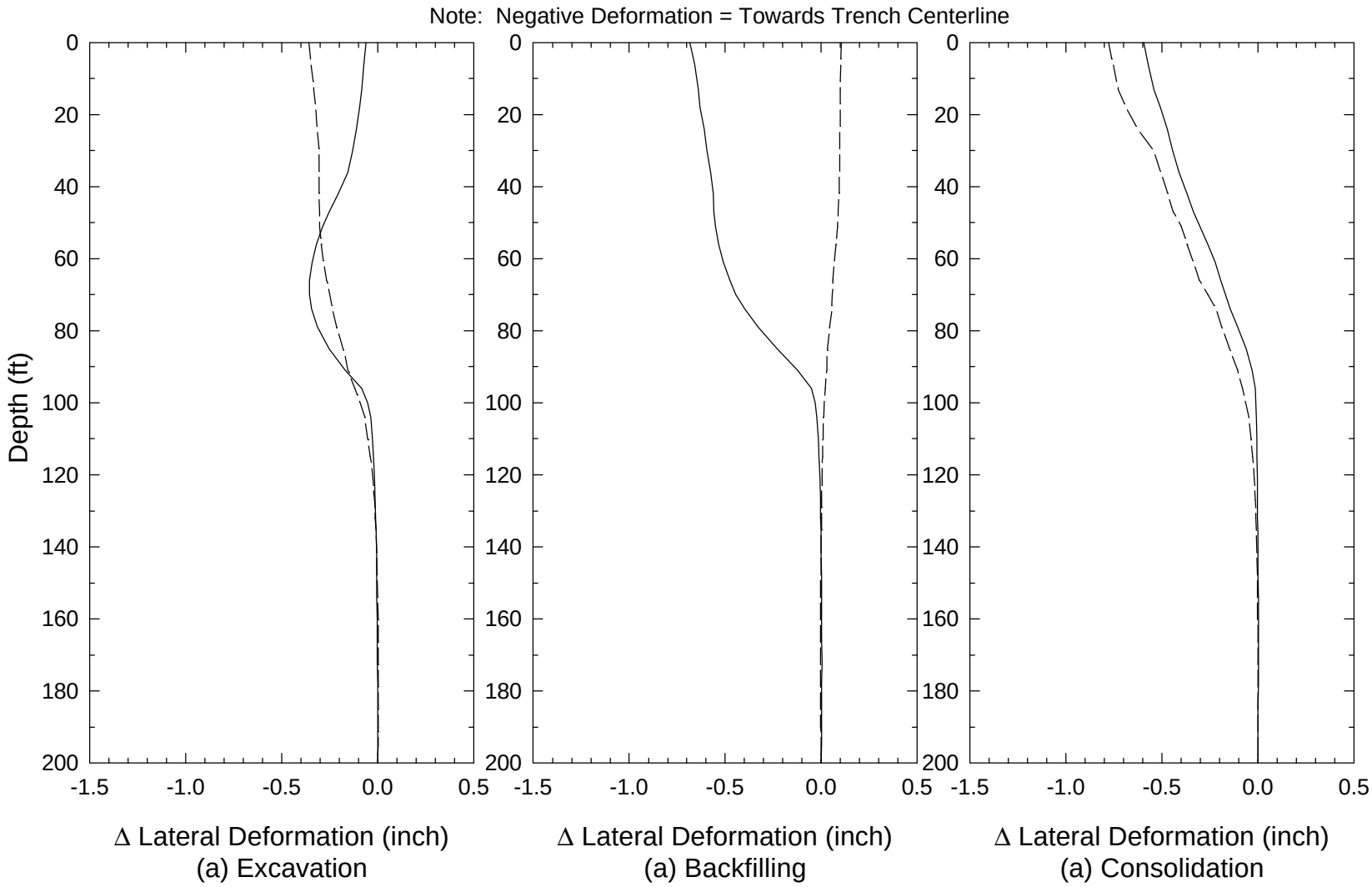

Figure 7.5 Base Case: Incremental Lateral Deformation at a Distance of 27 ft from Trench Centerline

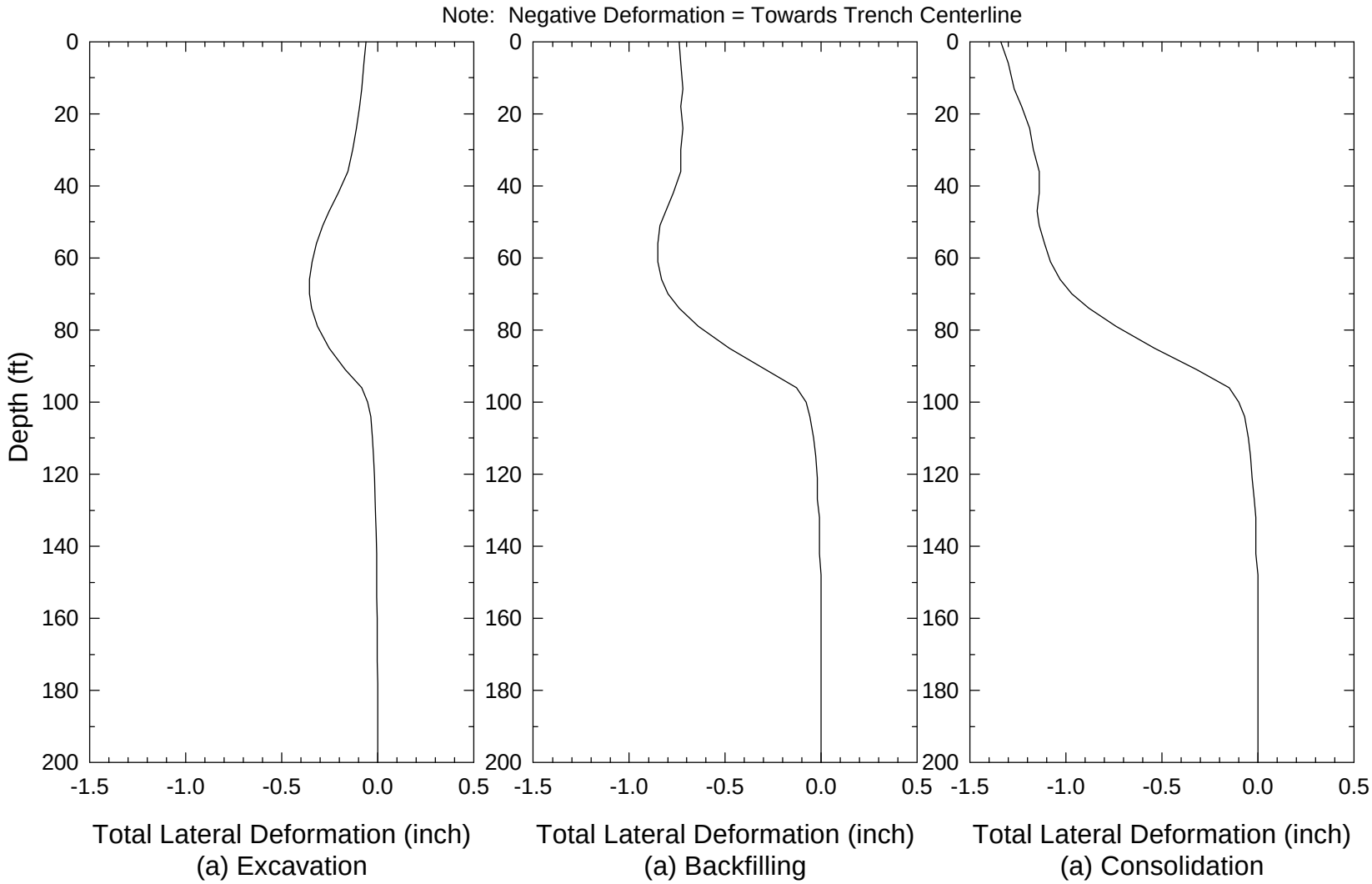

Figure 7.6 Base Case: Total Lateral Deformation at a Distance of 27 ft from Trench Centerline

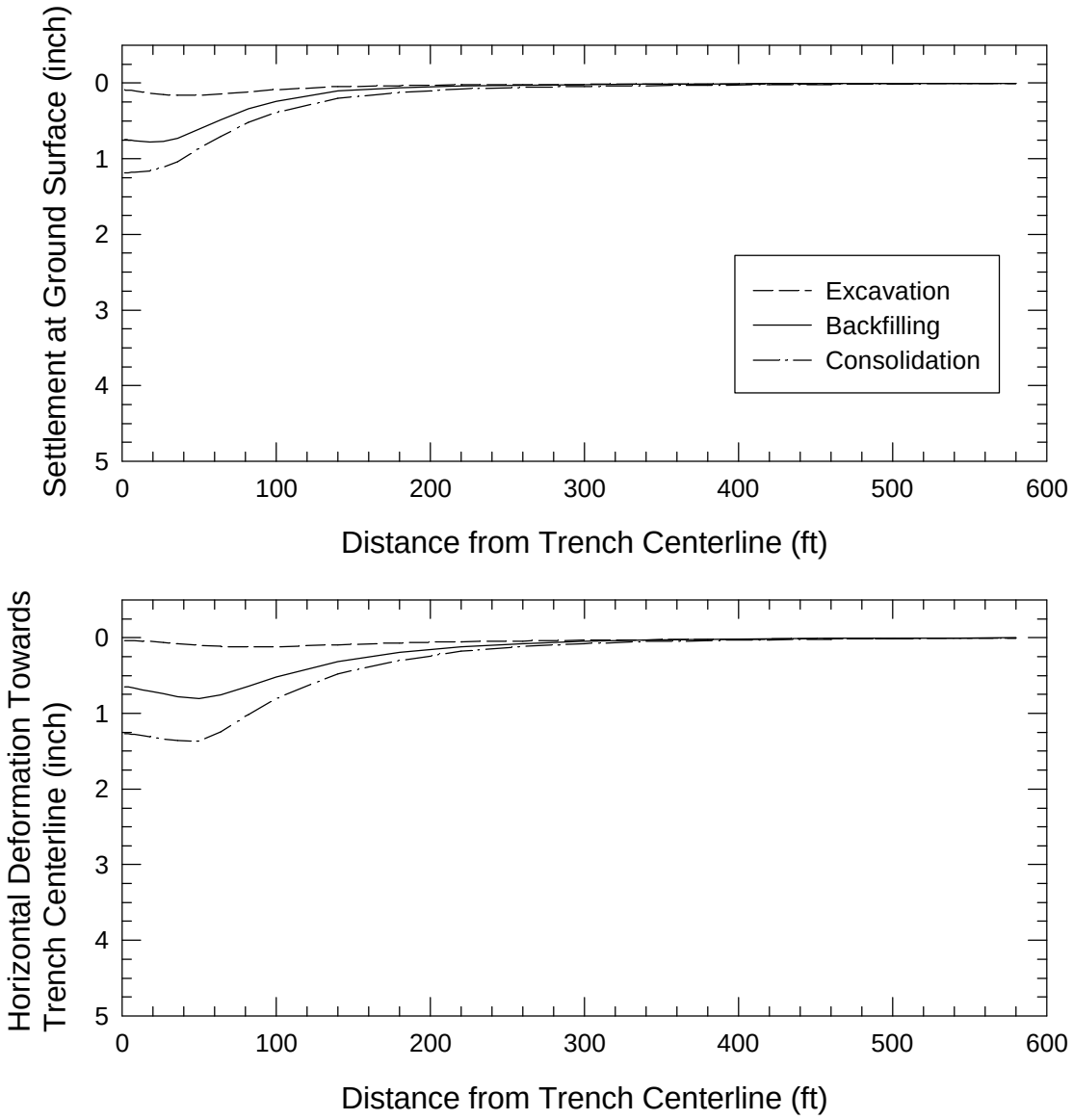

Figure 7.7 Base Case: Deformation at Ground Surface

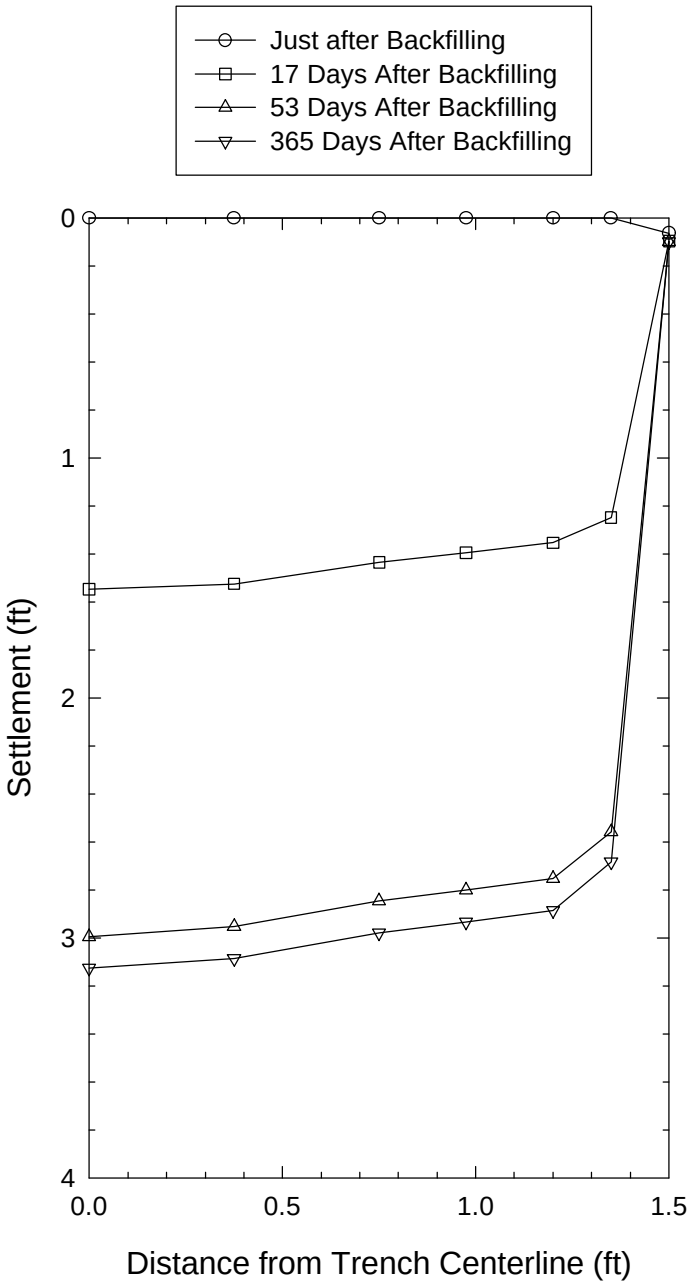

Figure 7.8 Base Case: Settlement in Soil-Bentonite Trench

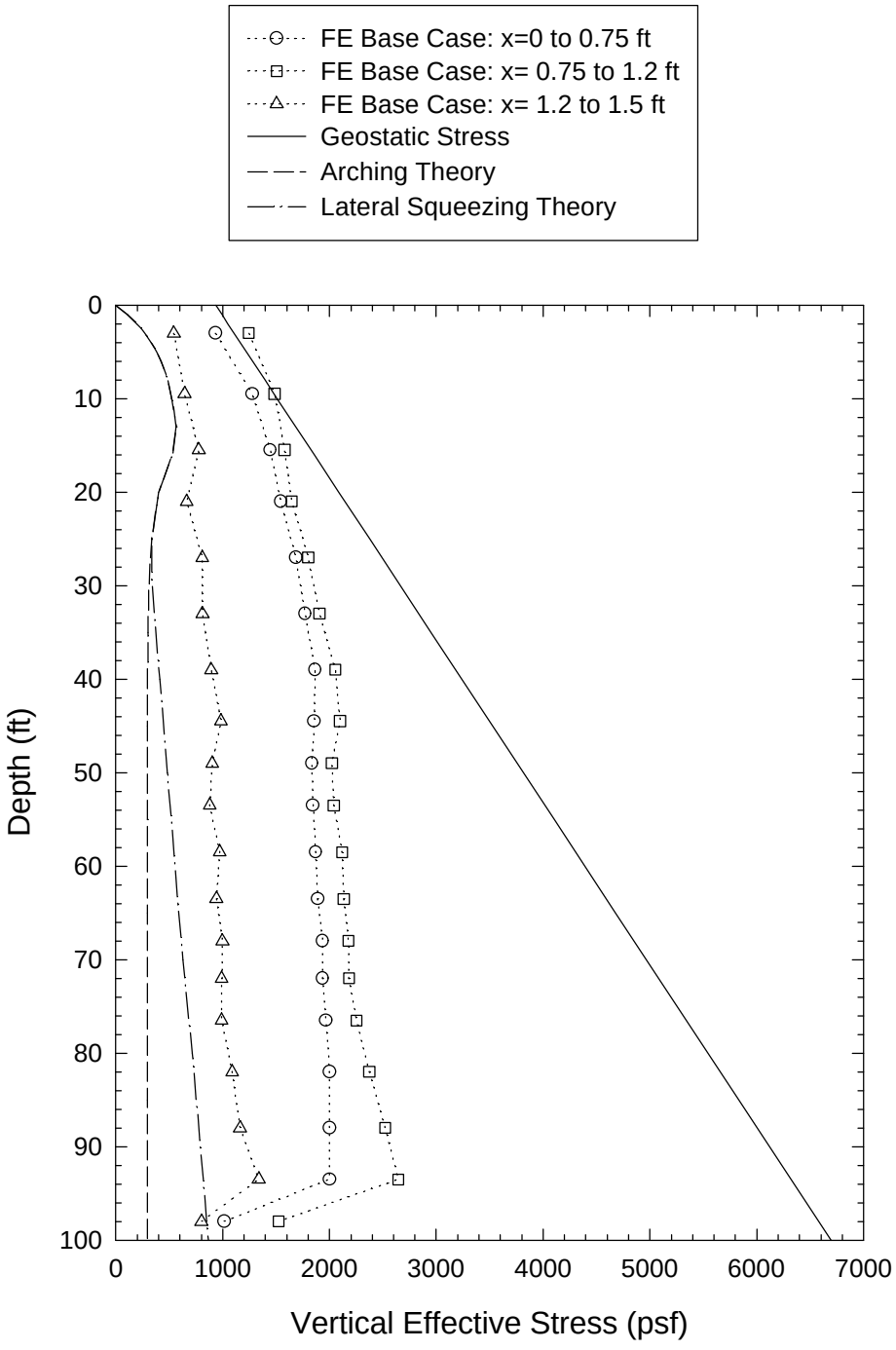

Figure 7.9 Vertical Effective Stress in Consolidated Soil Bentonite

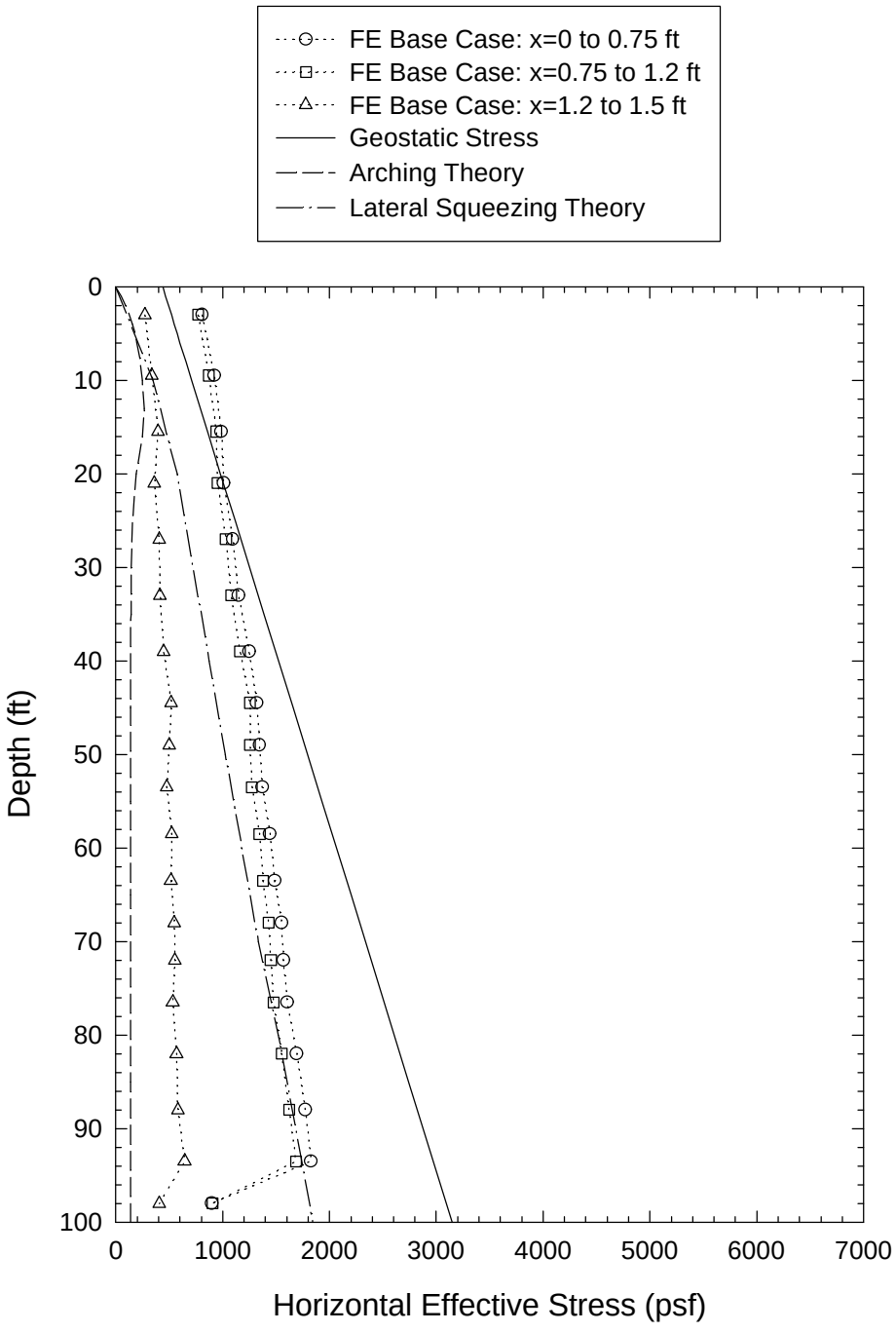

Figure 7.10 Horizontal Effective Stress in Consolidated Soil Bentonite

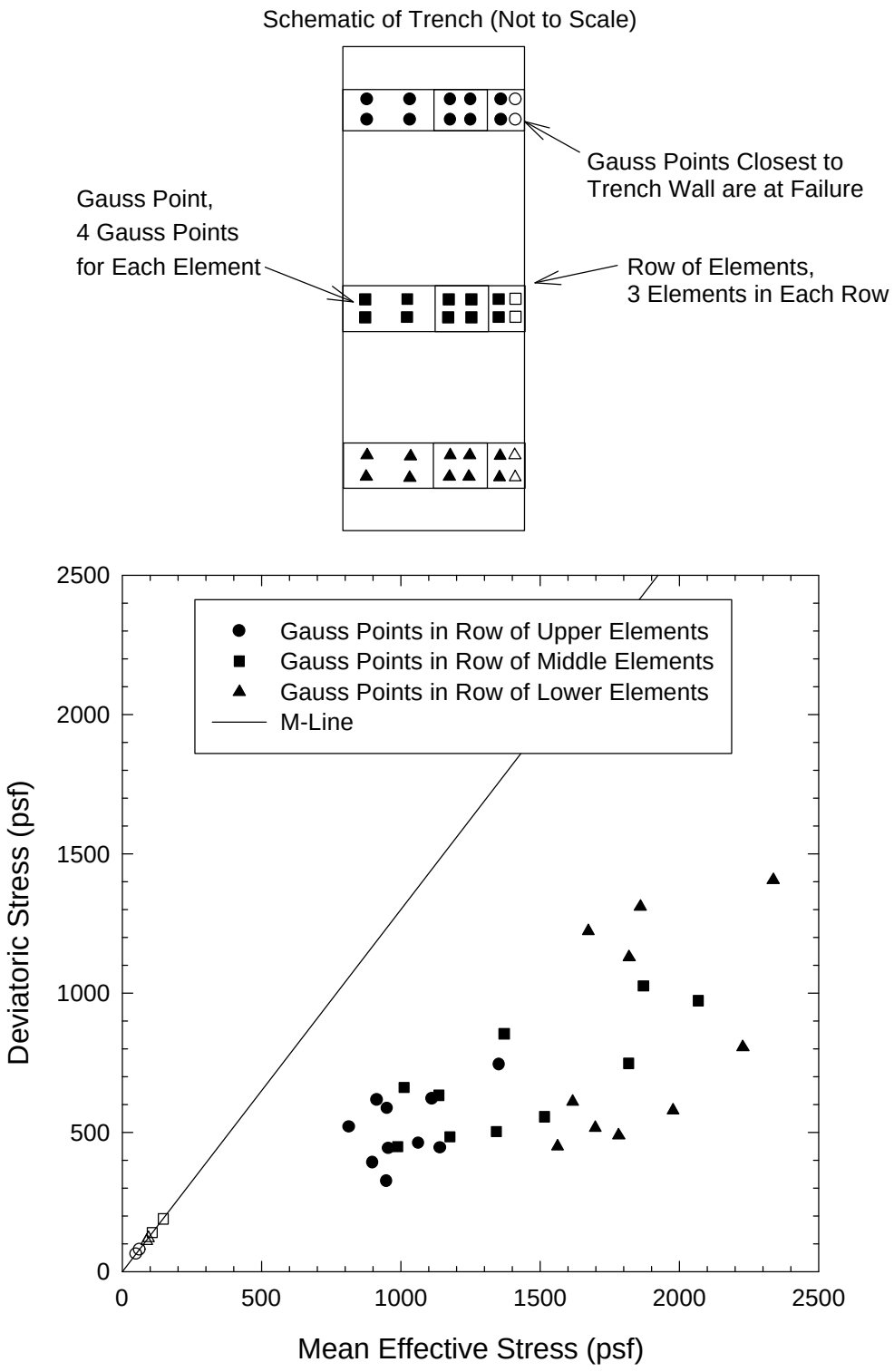

Figure 7.11 Stress State for Selected Gauss Points in Consolidated Soil-Bentonite

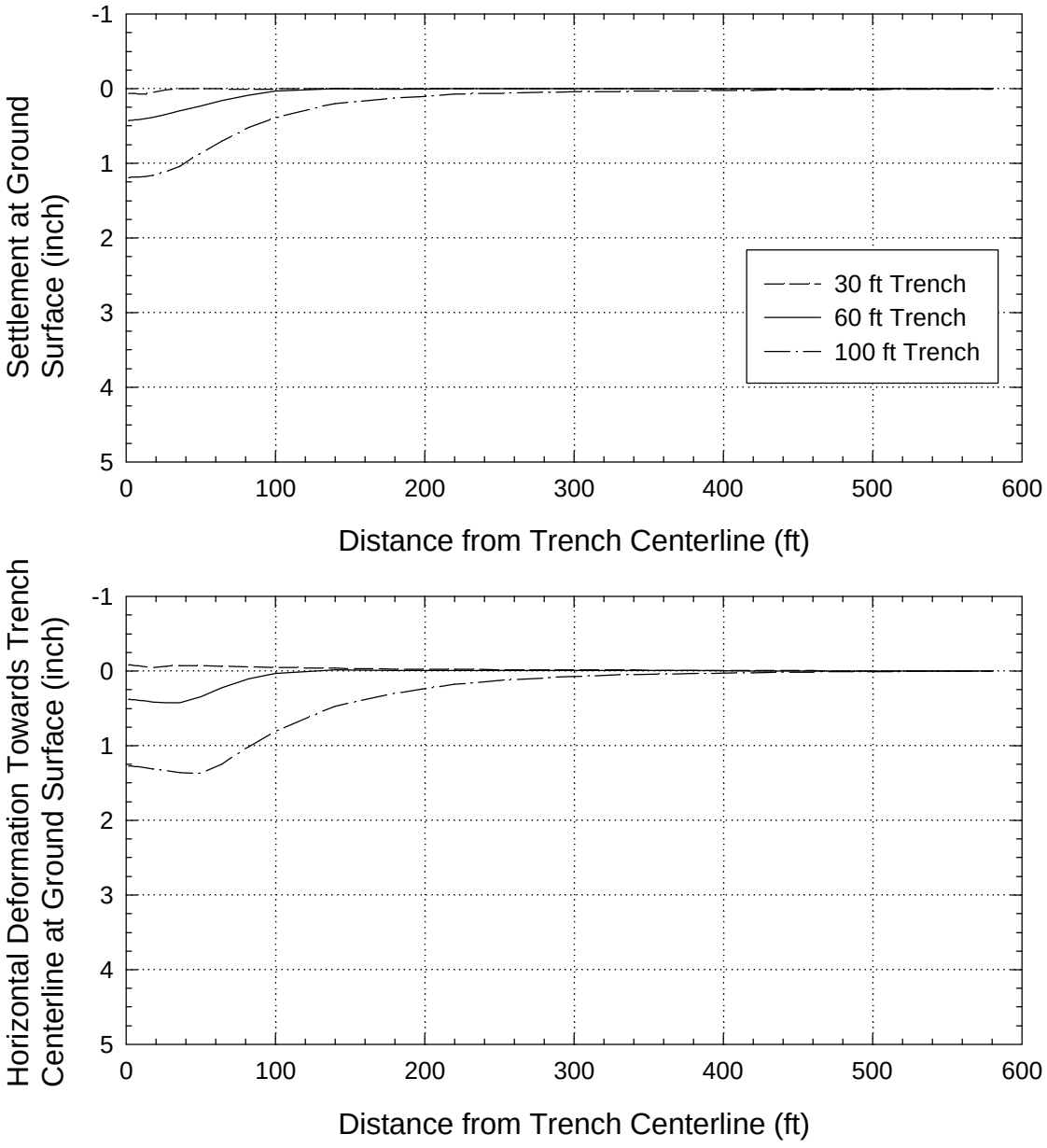

Figure 7.12 Effect of Trench Depth on Deformations in Adjacent Ground

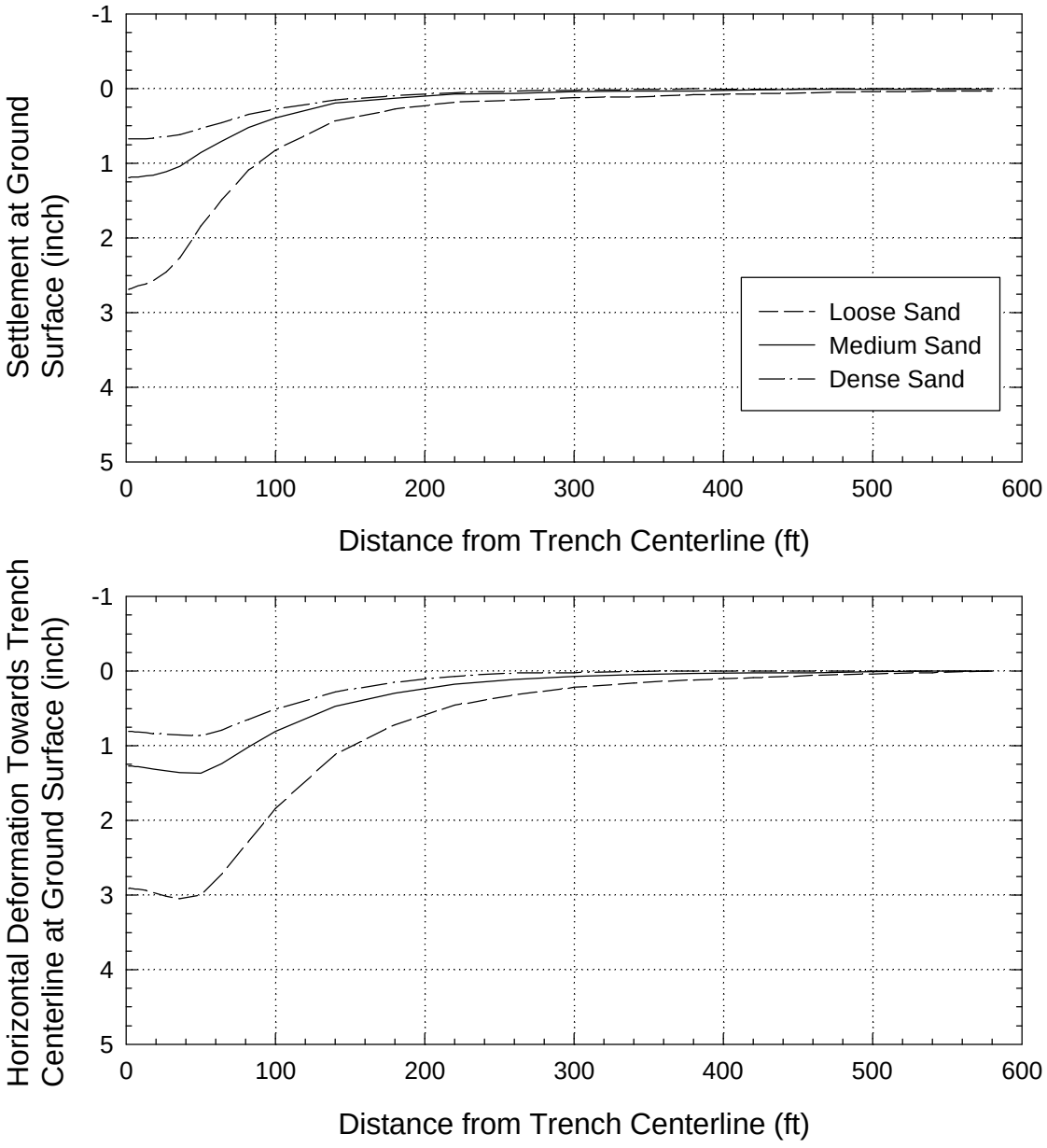

Figure 7.13 Effect of Sand Density for OCR=1 on Deformations in Adjacent Ground

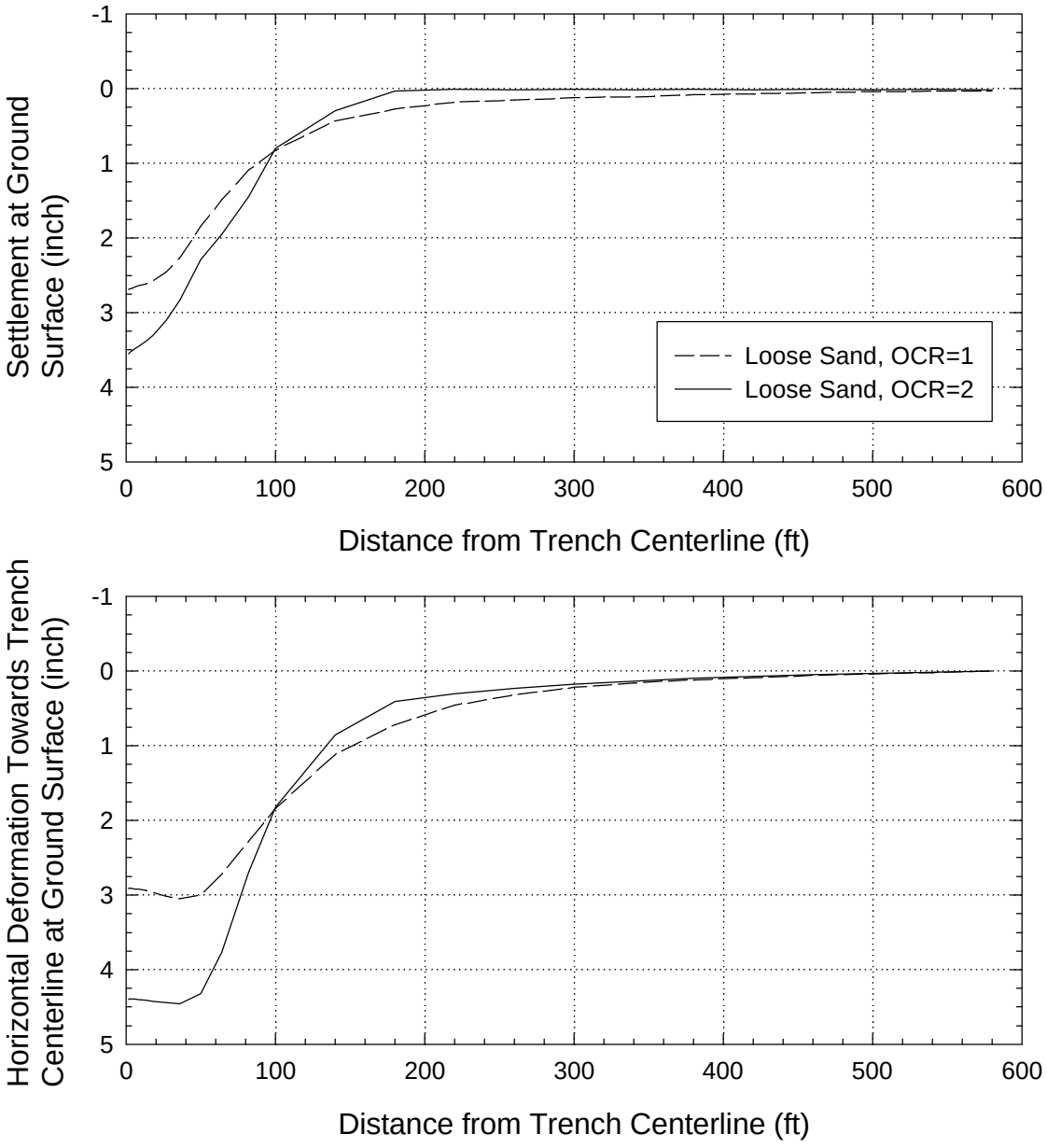

Figure 7.14 Effect of OCR of Loose Sand on Deformations in Adjacent Ground

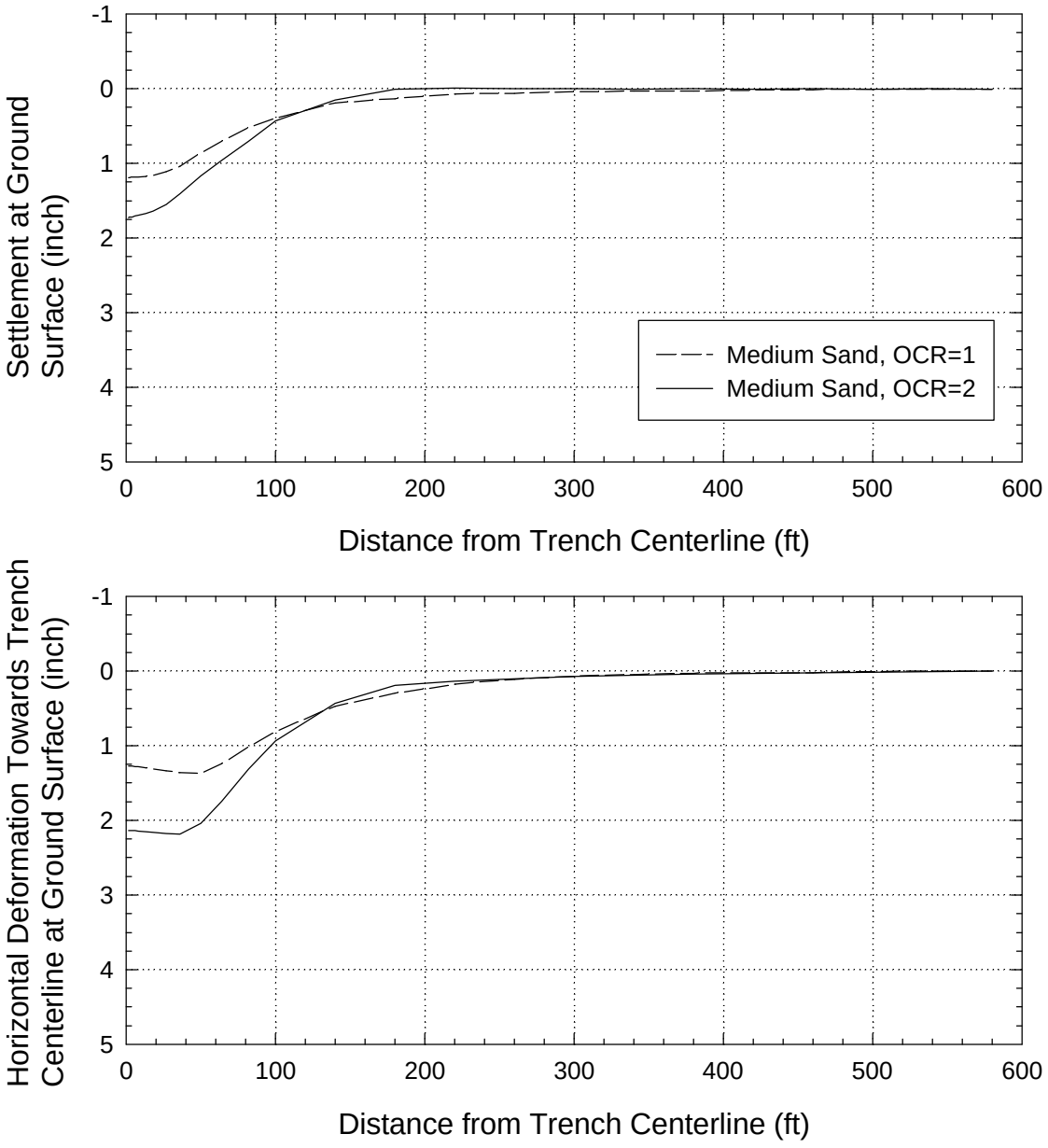

Figure 7.15 Effect of OCR of Medium Sand on Deformations in Adjacent Ground

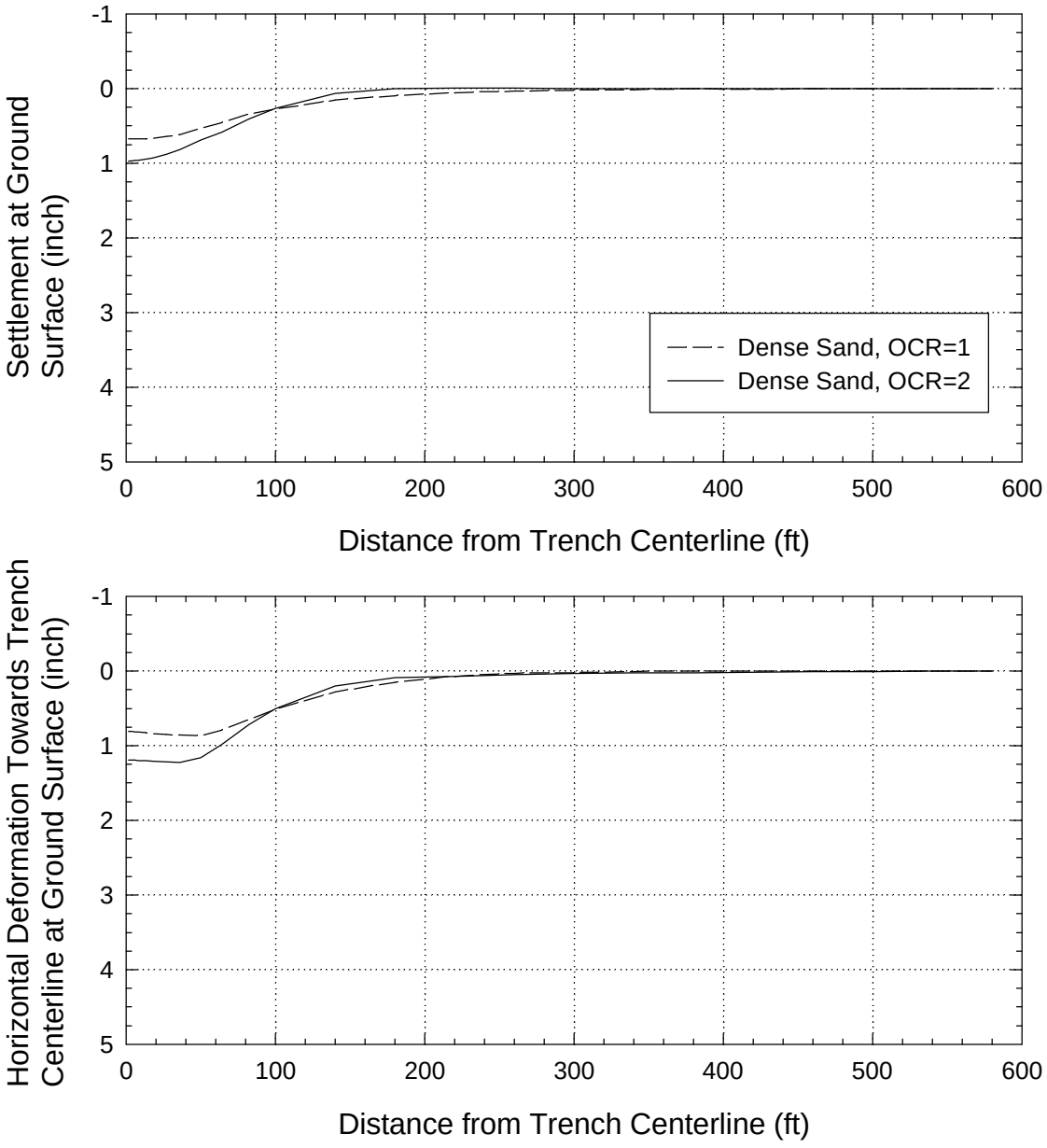

Figure 7.16 Effect of OCR of Dense Sand on Deformations in Adjacent Ground

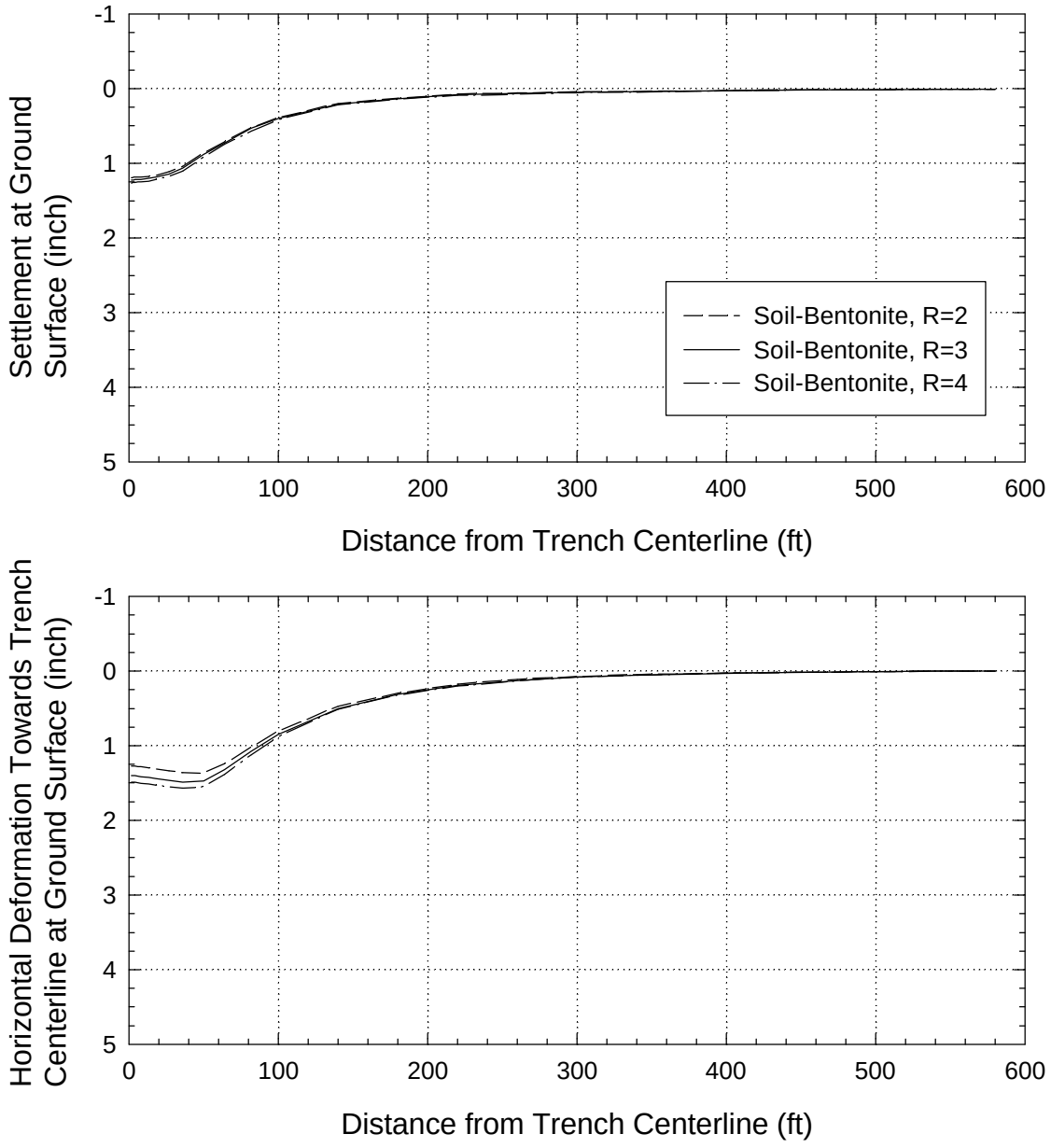

Figure 7.17 Effect of Soil-Bentonite R Parameter on Deformations in Adjacent Ground

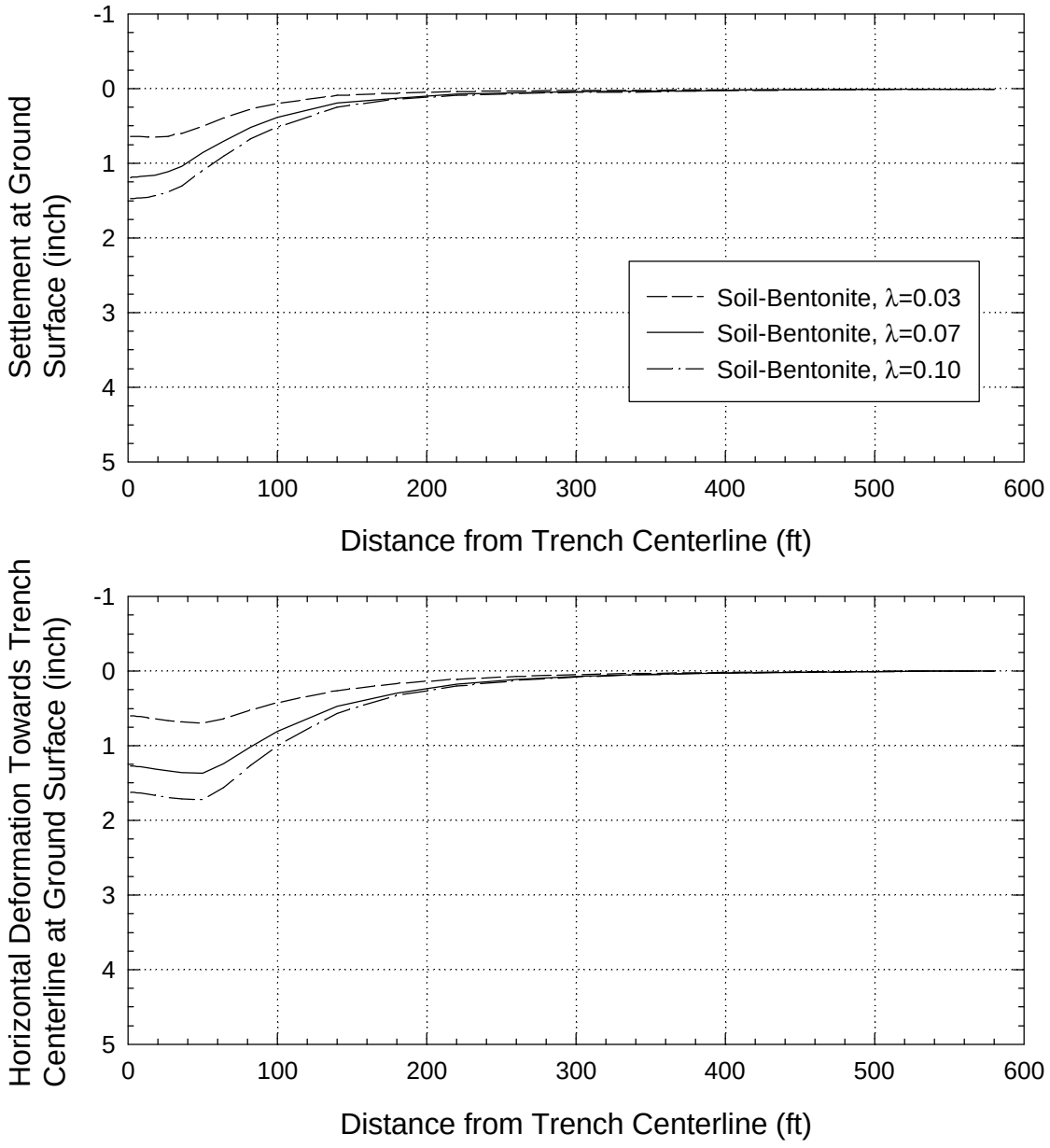

Figure 7.18 Effect of Soil-Bentonite λ Parameter on Deformations in Adjacent Ground

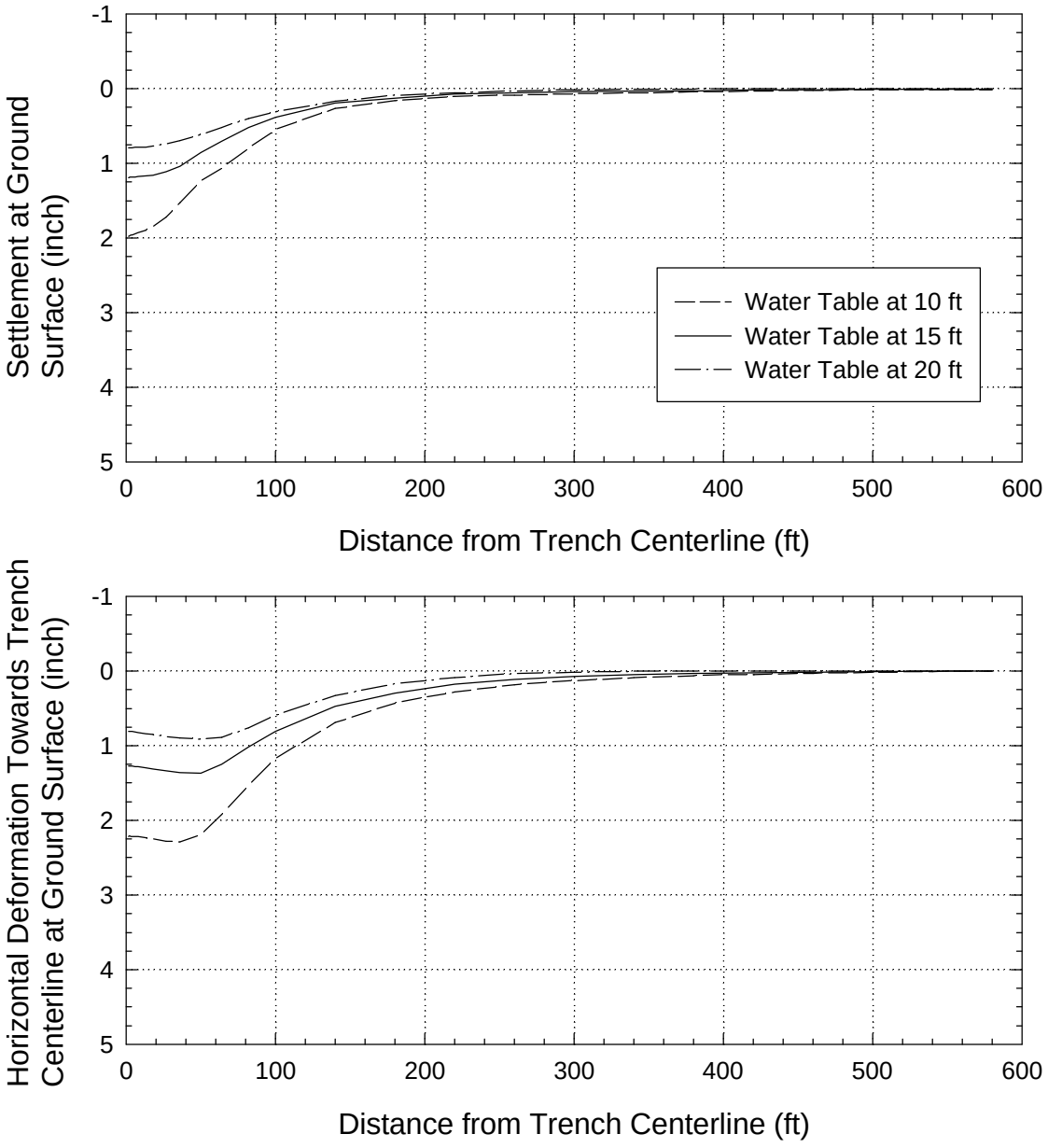

Figure 7.19 Effect of Water Table on Deformations in Adjacent Ground

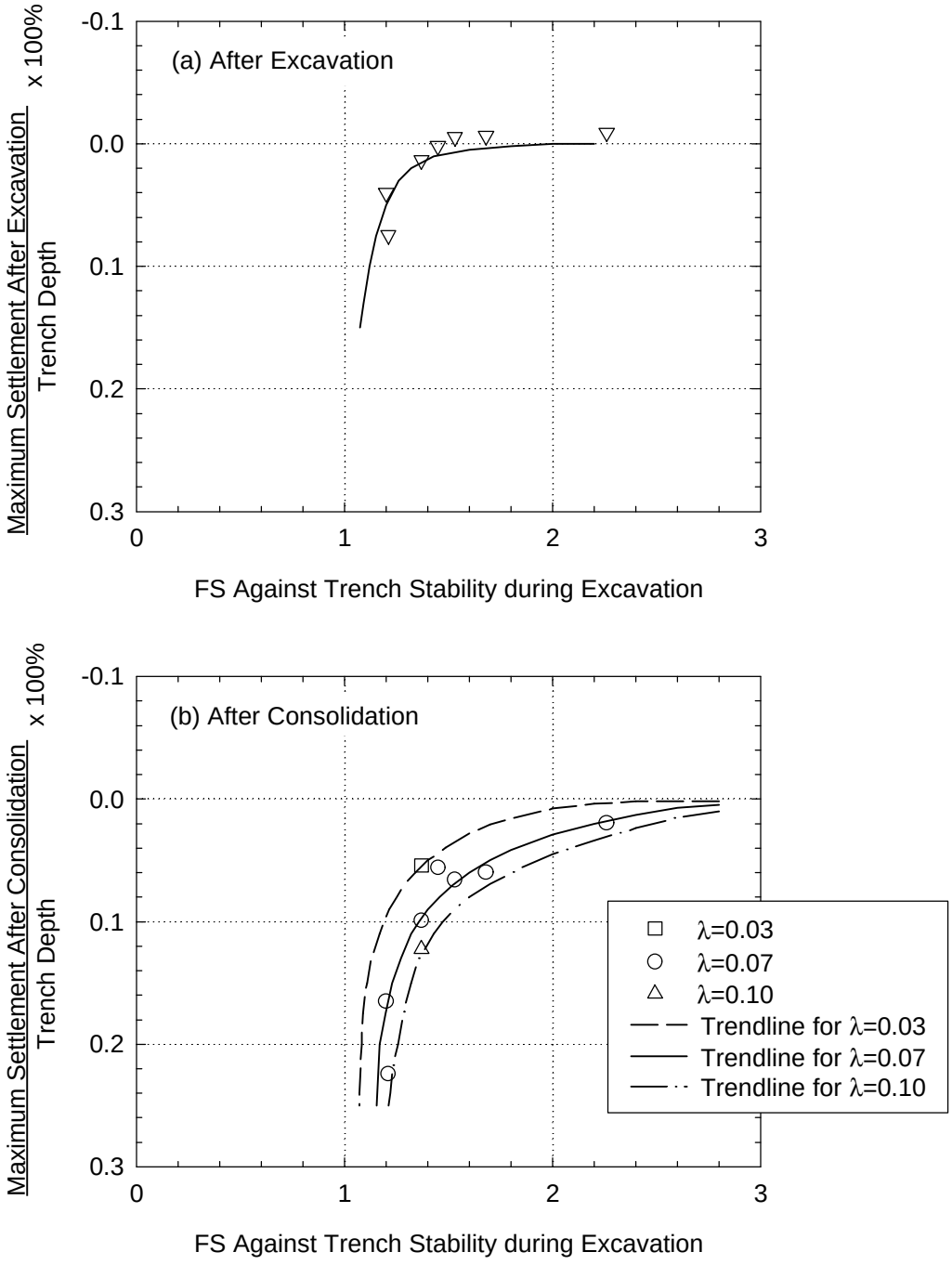

Figure 7.20 Normalized Maximum Settlement versus Factor of Safety Against Trench Stability during Excavation